Trimethyltriazacyclohexane Coordination Chemistry of Simple Rare-Earth Metal Salts

Journal:	*Dalton Transactions*
Manuscript ID	DT-ART-01-2023-000242.R2
Article Type:	Paper
Date Submitted by the Author:	13-Mar-2023
Complete List of Authors:	Wedal, Justin; University of California Irvine, Chemistry Ziller, Joseph; University of California, Irvine, Department of Chemistry Evans, William; University of California- Irvine, Department of Chemistry

Trimethyltriazacyclohexane Coordination Chemistry of Simple Rare-Earth Metal Salts

Justin C. Wedal, Joseph W. Ziller, and William J. Evans*

Department of Chemistry, University of California Irvine, Irvine, CA 92617, United States

Email: wevans@uci.edu

* To whom correspondence should be addressed.

Abstract

Reactions of 1,3,5-trimethyl-triazacyclohexane (Me_3tach) with common rare-earth iodide, chloride, and triflate salts were examined to determine the capacity of this inexpensive chelate to provide alternative precursors for THF-free reactions. The reaction of $LaI_3(THF)_4$ and $CeI_3(THF)_4$ with 1,3,5-trimethyl-triazacyclohexane in THF generated toluene soluble $(Me_3tach)_2LnI_3$, **1-Ln**, in which the Ln center has a tri-capped trigonal prismatic geometry with two eclipsed Me_3tach rings. Reaction with $NdI_3(THF)_{3.5}$ forms the analogous **1-Nd**, but a different structure with one outer sphere iodide, $[(Me_3tach)_2NdI_2][I]$, **2-Nd**, is also accessible and has a structure reminiscent of bent metallocenes. The reaction of $LaCl_3$ and Me_3tach forms the less soluble $(Me_3tach)_2LaCl_3$, which has a structure analogous to **1-Ln** with eclipsed Me_3tach rings. The mono-ring complex, $(Me_3tach)YCl_3(THF)_2$, could be isolated from the reaction of YCl_3 with Me_3tach. Reactions of $La(OTf)_3$ with Me_3tach were sensitive to the presence of residual proton sources as exemplified by the isolation of $\{[(Me_3tach)La(\mu\text{–}OH)(\mu\text{–}OTf)]_2(\mu\text{–}OTf)_2\}_2$, **5-La**, and $[HMe_3tach][(Me_3tach)_2La(OTf)_4]$, **6-La**. SmI_2 reacts with Me_3tach to produce the Sm(II) complex, $(Me_3tach)_2SmI_2(THF)$, **7-Sm**, but **2-Sm** can also form in this reaction. Complexes of the larger 1,4,7-trimethyltriazacyclononane (Me_3tacn) ligand, namely $(Me_3tacn)LaI_3(THF)$, $(Me_3tacn)YCl_3$, and $(Me_3tacn)SmI_2(THF)$ were synthesized for comparison. Several examples of

the protonated ligands with simple counteranions, [HMe$_3$tach][X] (X = Cl, Br, I) and [HMe$_3$tacn][OTf], were identified in the course of these studies.

Introduction

The development of the chemistry of the large electropositive rare-earth metals has been aided greatly by the use of cyclopentadienyl ligands, $(C_5R_5)^{1-}$ (R = H, alkyl, aryl).[1–3] Three of these monoanionic, six-electron donor ligands can react with metal trihalides to provide charge balance to the large Ln(III) ions while generating a formally nine-coordinate, sterically saturated neutral $(C_5R_5)_3Ln$ product (Ln = rare-earth metal). Metallocene complexes with two cyclopentadienyl ligands, $(C_5R_5)_2LnX(L)$ (X = anion; L = neutral ligand), are heavily studied to explore the chemistry of a single Ln–X bond in the presence of these large ancillary ligands that stabilize the metal ion both sterically and electrostatically.

In contrast, neutral, chelating, six-electron donor ligands like the cyclic, trisubstituted 1,3,5-trimethyl-1,3,5-triazacyclohexane, Me$_3$tach, and 1,4,7-trimethyl-1,4,7-triazacyclononane, Me$_3$tacn, compounds, Scheme 1, have received less attention with the rare-earth metals because they do not provide charge balance. They have been employed much more extensively with transition and main group metals[4-23] where electrostatic stabilization of a high oxidation state

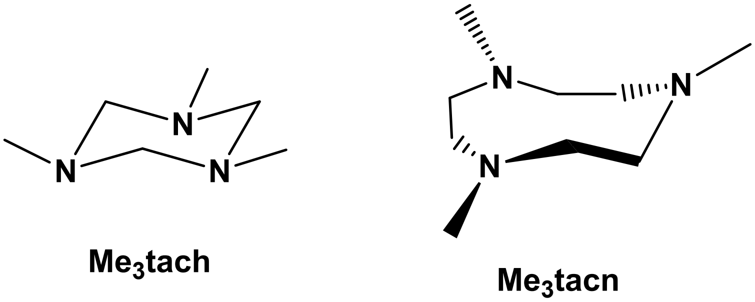

Scheme 1: Molecular structures of Me$_3$tach (left) and Me$_3$tacn (right).

cation is less important. With the transition and main group metals, the Me_3tacn ligand[4,5,14–18,6–13] has been studied more than the Me_3tach ligand,[4,19–23] although the latter is less expensive.

In the rare-earth metal area, the triazacycloalkanes mentioned above have been used to stabilize cationic complexes,[24–28] to provide a large neutral ligand that enhances the stability of polyalkyl complexes,[29–37] and to break up polymeric species to monometallic compounds.[38] Interestingly, Mitzel and coworkers found that small changes in the size of the rare-earth metal can lead to large changes in the reaction chemistry of R_3tach complexes. For example, reaction of $Sm(AlMe_4)_3$ with $^iPr_3$tach led to reduction of the samarium center and formation of $(^iPr_3tach)_2Sm(AlMe_4)_2$,[37] but addition of the same ligand to the smaller metal compound $Y(AlMe_4)_3$ led to deprotonation of a methyl group and formation of the methylidene complex $(^iPr_3tach)Y(AlMe_4)(Me_3AlCH_2AlMe_3)$.[31] Currently, the number of rare-earth metal compounds with R_3tach ligands reported in the literature is limited to these examples: Sc (R = Me),[30] Y (R = Me, ^{i}Pr, Cy),[30–33,39] La (R = Me),[33,35,40] Ce (R = Me),[36] Pr (R = Me, Et),[34,35] Nd (R = Me),[38,40] Sm (R = Me, Et, ^{i}Pr, ^{t}Bu, Cy),[29,33,37] Tb (R = Me),[38] and Ho (R = Me). Examples of rare-earth metal complexes with the larger Me_3tacn ligand are limited to a single crystallographically characterized example for La,[41] Nd,[38] Gd,[42] and Tb,[38] and many examples with Sc[26,30]and Y.[26,30]

One area of rare-earth metal triazacycloalkane chemistry that has not received much attention is the coordination chemistry of these chelates with simple rare-earth metal salts that function as common starting materials for numerous reactions. We were interested in the potential for Me_3tach to form soluble precursors that would be useful in THF-free reactions. We report here on our initial studies with rare-earth metals that has already been extended to U, Np, and Pu chemistry[43] and to a study of Me_3tach with bismuth halides.[44] The present coordination chemistry survey of Me_3tach with rare-earth metal starting materials focuses on La(III) salts to make comparisons between iodide, chloride, and triflate complexes, as well as Me_3tach and Me_3tacn comparisons. Results with some other Ln(III) ions are included as well as some SmI_2 reactions.

Results

Reaction of Me_3tach with $LnI_3(THF)_x$. Addition of two equivalents of Me_3tach to $LnI_3(THF)_4$ (Ln = La, Ce) in THF generated toluene soluble $(Me_3tach)_2LnI_3$, **1-Ln**, eqn (1). **1-Ln** were characterized by X-ray diffraction studies, Fig. 1, and NMR spectroscopy, see ESI for complete details. Briefly, the ^{1}H NMR spectrum for diamagnetic **1-La** in THF-d_8 displayed three resonances in a 6:6:18 ratio which is attributed to magnetically inequivalent methylene protons and the methyl groups, respectively. The methylene resonances were poorly resolved and appeared as a broadened singlet, which could be due to fluxional behavior on the NMR timescale. Similar resonances were observed for **1-Ce** and the previously reported uranium and bismuth Me_3tach compounds.[43,44] We find that some diamagnetic rare-earth metal compounds containing R_3tach ligands have well-resolved NMR spectra and others do not.[30-40]

Each **1-Ln** complex has the LnI_3 unit sandwiched between two Me_3tach ligands. These molecular structures are analogous to the U, Np, and Pu actinide complexes $(Me_3tach)_2AnI_3$, **1-An**.[43] However, only **1-U** is isomorphous with **1-Ln**, since **1-Np** and **1-Pu** crystallize with THF in the lattice and the **1-Ln** complexes do not. Notably, compound **1-La** also formed only when one equivalent of Me_3tach was added to the reaction. This tendency to form bis(Me_3tach) complexes has been previously observed in the reaction of one equivalent of Me_3tach with $Pr(OTf)_3$ which formed $(Me_3tach)_2Pr(OTf)_3$.[34]

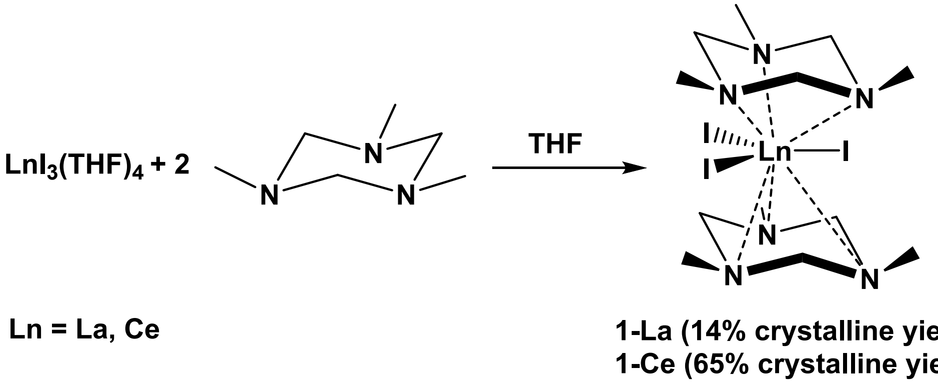

(1)

In contrast to **1-U**,[39] the crystal data of these **1-Ln** complexes were not of sufficient quality to discuss metrical parameters but did confirm the connectivity of the molecule. In each case, the metal and three iodine atoms reside on a mirror plane, such that only one Me_3tach moiety is unique and the other is generated by symmetry. The coordination geometry for **1-Ln** can be described as tricapped trigonal prisms, where the two Me_3tach rings are eclipsed and the iodides are staggered with respect to the Me_3tach nitrogen atoms. **1-La** and **1-Ce** are readily soluble in both THF and arenes. This feature makes them attractive for use as precursors in reactions that are sensitive to ethereal solvents.

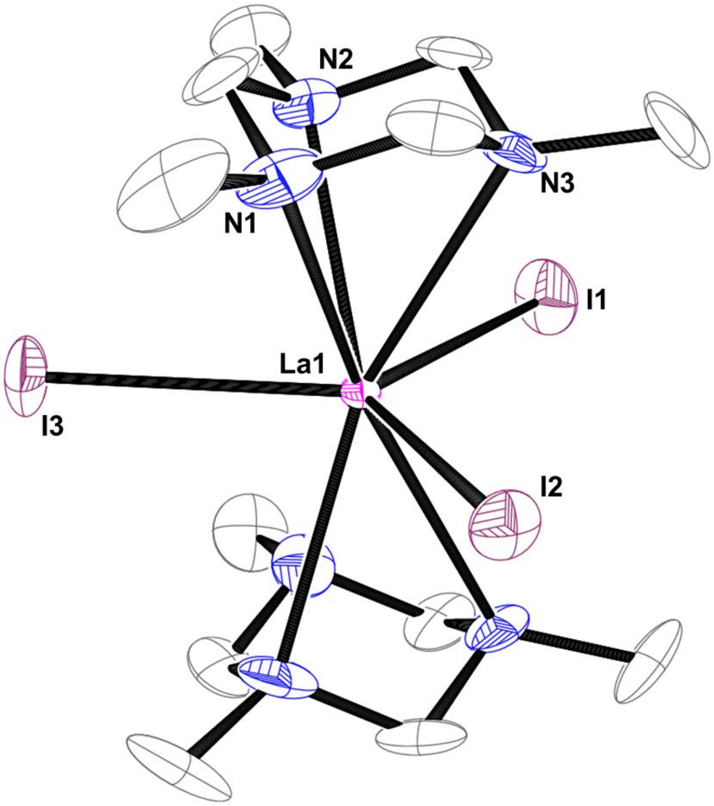

Fig. 1 Connectivity structure of **1-La** with selective atom labelling. Hydrogen atoms have been omitted for clarity. **1-La**, **1-Ce**, and **1-Nd** are isomorphous and all structures were connectivity only.

The addition of two equivalents of Me_3tach to $NdI_3(THF)_{3.5}$ in THF generates two different sets of crystals that were observed under the microscope, eqn (2). Complex **1-Nd**, which is isomorphous with **1-La** and **1-Ce,** has the parallel-ring sandwich structure shown in Fig. 1. The other complex was identified as $[(Me_3tach)_2NdI_2][I]$, **2-Nd**, which has a bent ring structure with one outer-sphere iodide, Fig. 2. The observation of two unique structures from the same crystallization conditions suggests that both of these structures are close in energy.[45–47] The neodymium center in **2-Nd** is eight-coordinate and has a structure reminiscent of bent metallocenes such as $(C_5Me_5)_2LnX(L)$ and $[(C_5Me_5)_2LnX_2]^{1-}$ (X = anion; L = neutral ligand).[48] Like the data on **1-Ln**, the crystal data for both **1-Nd** and **2-Nd** were not of high enough quality to discuss metrical parameters. The mixture of both neodymium complexes was readily soluble in THF, but appears only sparingly soluble in toluene, likely due to the structure of **2-Nd** having an outer sphere iodide.

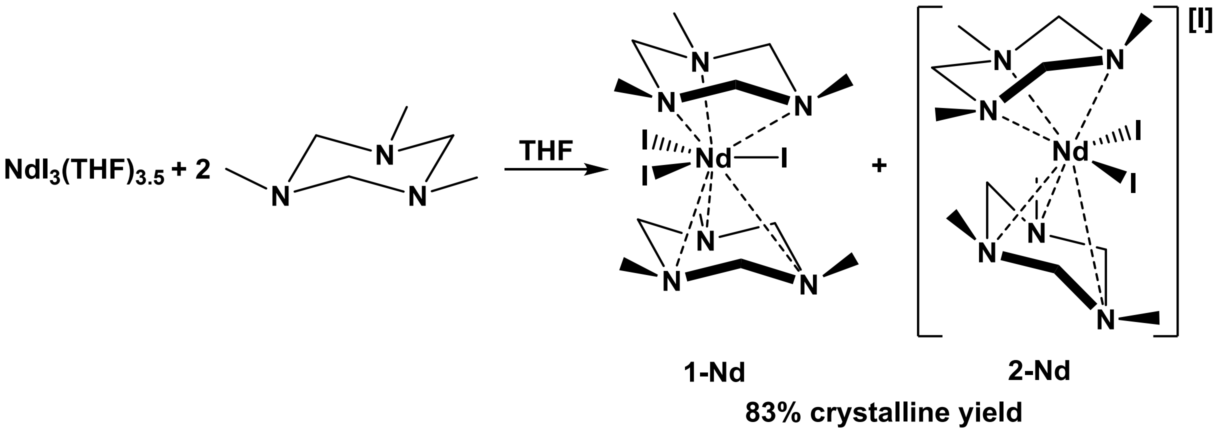

(2)

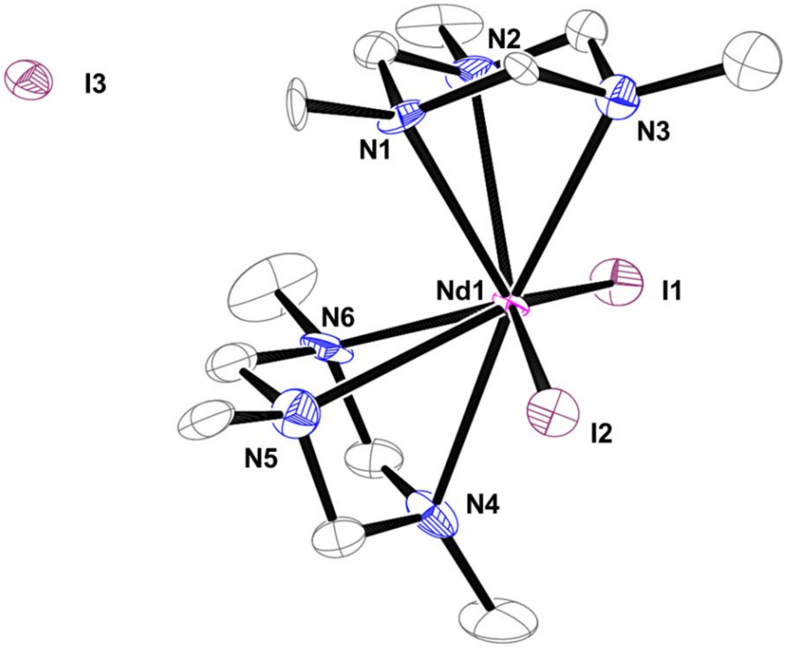

Fig. 2 Connectivity structure of **2-Nd** with selective atom labelling. Hydrogen atoms have been omitted for clarity.

Reaction of Me_3tach with $LnCl_3$. When the reaction of Me_3tach with $LaCl_3$ was examined, the complex $(Me_3tach)_2LaCl_3$, **3-La**, eqn (3), was isolated, Fig. 3. The structure of

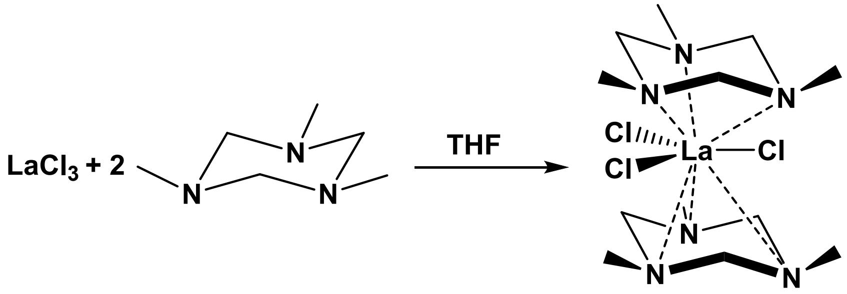

(3)

3-La
8% crystalline yield

3-La is analogous to those of **1-Ln** and can also be described as a tricapped trigonal prism with parallel Me_3tach ligands and face-capping chlorides. In contrast to the toluene soluble **1-Ln** complexes, **3-La** does not readily dissolve in toluene and is only sparingly soluble in THF which results in a very low isolated yield, eqn (3). As a consequence, the chloride complexes appeared less useful for the preparation of soluble $(Me_3tach)_nLnX_3$ complexes. The ^1H NMR spectrum of **3-La** in THF-d_8 only displayed one broad resonance, likely due to the poor solubility of the compound.

3-La crystallizes in the $P6_3/m$ space group such that only the La, one Cl, one N, and two C atoms were observed in the crystal data and the rest of the molecule was generated by symmetry. Hence, **3-La** has only one unique value for the La–Cnt, La–N, and La–Cl distances, where Cnt is defined as the calculated centroid of the three nitrogen donor atoms.[43,44] As a result of the symmetry, the Cnt–La–Cnt angle in **3-La** is exactly 180°, the Cnt–La–Cl angle is 90°, and the Cl–La–Cl angle is 120°. The La–Cnt distance in **3-La** is 2.428 Å. These values are summarized in Table 1 and full data can be found in the ESI. A comprehensive table of rare-earth metal complexes containing R_3tach and R_3tacn ligands can be found in the ESI, along with the corresponding M–Cnt distances. When the ionic radius[49] of each metal is accounted for, there is only a slight deviation in the M–Cnt distances that can likely be explained by the difference in the steric size of the R substituents and the overall coordination number of the complex.

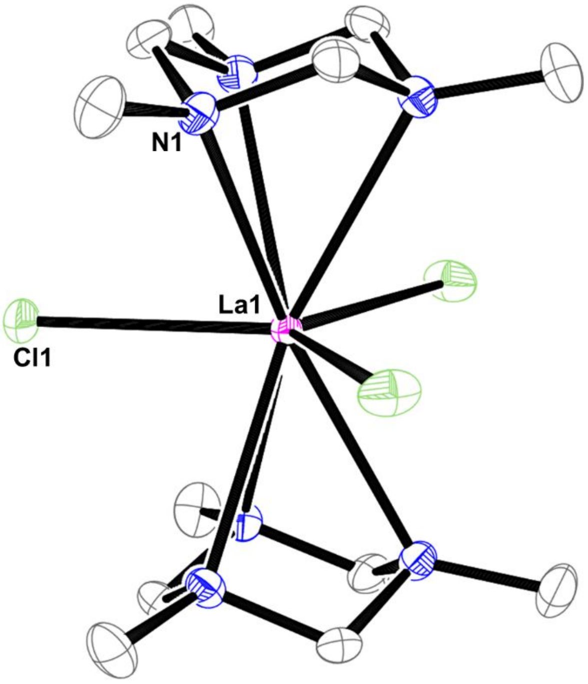

Fig. 3 Molecular structure of **3-La** with selective atom labelling. Ellipsoids are drawn at the 50% probability level and hydrogen atoms have been omitted for clarity.

Table 1 Selected distances (Å) and angles (°) for **3-La**, **4-Y**, **5-La**, **6-La**, **8-La**, **9-Y**, and **10-Sm**. Cnt is the centroid defined by the three nitrogen atoms of the Me_3tach or Me_3tacn ring and X = Cl, I, O(OTf). See Table S1 for comparisons with related rare-earth metal Me_3tach compounds.

	Ln–Cnt	Ln–N	Ln–X	Ln–O(THF)	Cnt–Ln–Cnt	Cnt–Ln–X	Cnt–Ln–O(THF)
3-La	2.428	2.7759(8)	2.7878(4)		180.	90.	
4-Y	2.214	2.5661(15), 2.5881(16), 2.6138(15)4	2.6232(5), 2.6356(5), 2.6558(5)	2.4208(13), 2.4440(12)		97.1, 98.0, 104.6	105.8, 174.8
5-La	2.411, 2.419	2.752(4), 2.761(4), 2.761(4), 2.771(4), 2.777(4), 2.783(4)	2.510(3), 2.510(3), 2.530(3), 2.537(3), 2.551(3),			76.7, 81.6, 83.2, 87.1, 90.6, 93.4,	

			2.588(3), 2.620(3)			93.4, 104.7	
6-La	2.449, 2.454	2.774(3), 2.778(3), 2.782(3), 2.795(3), 2.824(3), 2.842(3)	2.468(2), 2.525(2), 2.525(2), 2.579(2)		163.1	85.5, 87.0, 96.3, 99.6, 83.3, 86.8, 92.5, 97.9	
8-La	2.129	2.668(9), 2.744(8), 2.752(9)	3.1337(9), 3.1738(9), 3.1749(9)	2.628(6)		104.1, 105.3, 107.0	171.6
9-Y	1.848	2.483(5), 2.499(5), 2.508(5)	2.5555(17), 2.5592(17), 2.5610(17)			114.4, 117.3, 118.0	
10-Sm	2.065	2.640(7), 2.659(8), 2.699(8)	3.1789(11), 3.2012(10)	2.538(7)		117.6, 120.0	119.5

Me_3tach was also found to form a complex with the trichloride of a smaller metal, yttrium, but in this case a mono(Me_3tach) complex was obtained with two coordinated THF molecules. (Me_3tach)$YCl_3(THF)_2$, **4-Y**, was isolated from the reaction of two equivalents of Me_3tach to YCl_3 in THF after crystallization from THF/hexane eqn (4), Fig. 4. Compound **4-Y** displays a well-resolved ^{1}H NMR spectrum in THF-d_8. Like **1-Ln**, three resonances were observed attributable to inequivalent methylene protons and the methyl group, respectively. However, in **4-Y** the methylene protons appear as well-resolved doublets with a coupling constant of $J = 6.9$ Hz which is slightly lower than the other previously reported (R_3tach)Y compounds which range from 7.7–9.7 Hz.[31,32,35]

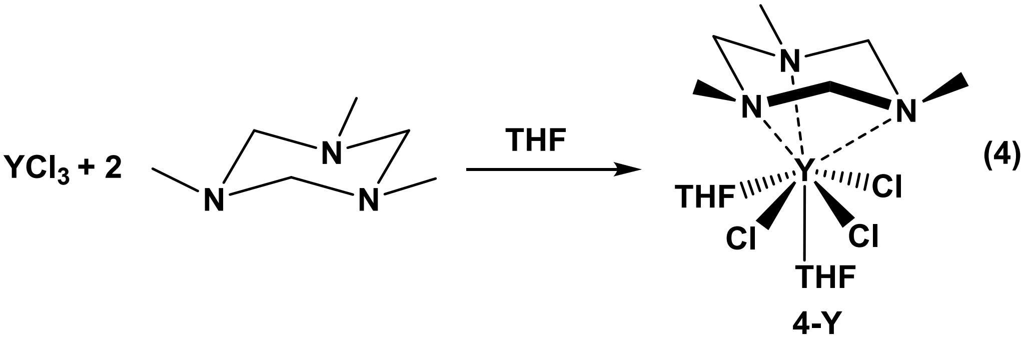

4-Y
92% crystalline yield

Compound **4-Y** crystallizes in the $P2_12_12_1$ space group as an eight-coordinate complex with two of the coordination sites occupied by THF. One THF is *trans* to the Me_3tach ring with a Cnt–Y–O(2) angle of 174.8°, Table 1. The *cis* THF has a 105.8° Cnt–Y–O(1) angle that differs from the 97.1, 98.0, and 104.6° Cnt–Y–Cl angles. The three chloride ligands and the O(1) donor atom are co-planar to within 0.001 Å and the yttrium atom lies 0.493 Å above the plane. The 2.214 Å Y–Cnt distance in **4-Y** is shorter than the 2.428 Å value in **3-La**, as expected for the smaller metal. The Y–Cnt distance in **4-Y** similar to the 2.223 and 2.229 Å distances in $[(Me_3tach)_2YMe_2][AlMe_4]$,[32] the 2.273 and 2.298 Å distances in $(Me_3tach)_2Y$(1,8-dialkynylanthracene)$_3$,[32] and the 2.160 and 2.171 Å distances in $(Me_3tach)_2Y(C{\equiv}CPh)_3$.[32] See Table S1 in the ESI for an exhaustive table.

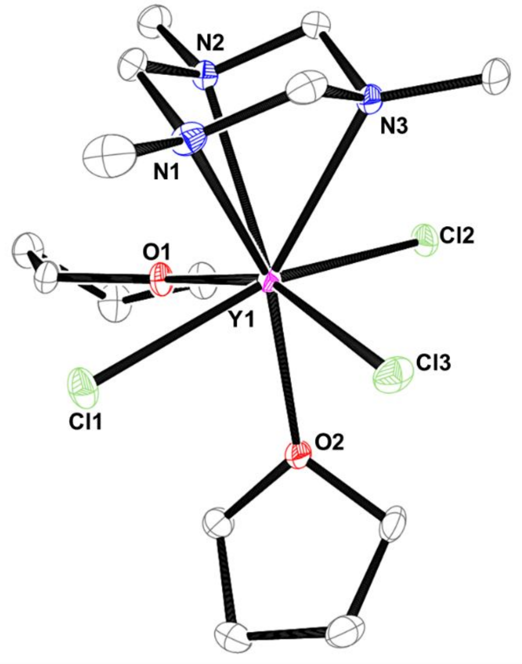

Fig. 4 Molecular structure of **4-Y** with selective atom labelling. Ellipsoids are drawn at the 50% probability level and hydrogen atoms have been omitted for clarity.

Reaction of Me_3tach with La(OTf)$_3$. The coordination chemistry of Me_3tach with lanthanum triflate was also investigated because rare-earth metal triflates (OTf) are also common starting materials. Previously, the reaction of Pr(OTf)$_3$ with Me_3tach was reported to form (Me_3tach)$_2$Pr(OTf)$_3$.[34] In an attempt to replicate this result with lanthanum and to compare with **1-La** and **3-La** above, La(OTf)$_3$ was reacted with two equivalents of Me_3tach in THF.

The initial reaction between La(OTf)$_3$ and Me_3tach led to the identification of the hydroxide compound $\{[(Me_3tach)La(\mu–OH)(\mu–OTf)]_2(\mu–OTf)_2\}_2$, **5-La**, by X-ray crystallography, Fig. 5. The tetrametallic **5-La** has two crystallographically independent La sites (e.g., La1 and La2 in Fig. 5) which are connected by two triflate and two hydroxide bridges. This bimetallic unit is bridged to its symmetry equivalent through two bridging triflate ligands. Overall, each lanthanum center is nine-coordinate. Metrical parameters involving La1 were slightly shorter than those involving

La2, see Table 1 and ESI for full details. The La–Cnt distances of 2.411 and 2.419 Å are similar to the 2.428 Å distance in **3-La**.

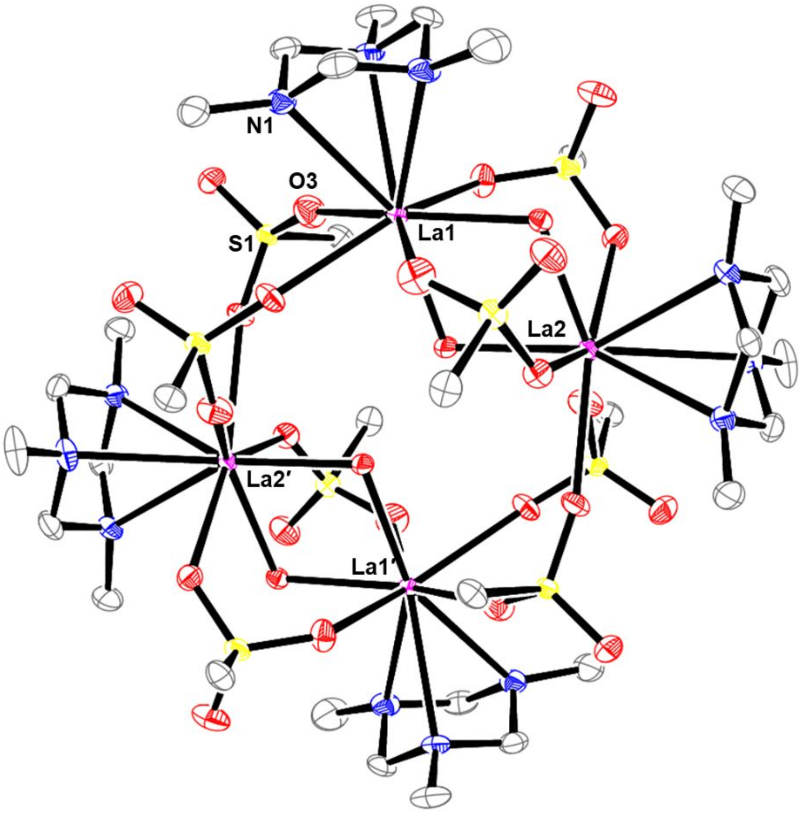

Fig. 5 Molecular structure of **5-La** with selective atom labelling. Ellipsoids are drawn at the 50% probability level. Hydrogen and fluorine atoms have been omitted for clarity.

The infrared spectrum of the La(OTf)$_3$ starting material contained two broad absorptions around 3300 cm^{-1}, likely indicating the presence of either H_2O, (OH)$^{1-}$, or residual HOTf. Subsequently, the La(OTf)$_3$ starting material was placed under vacuum at 10^{-6} Torr and heated at 100 °C overnight. The free-flowing white powder thus obtained showed no O–H stretches in the infrared spectrum. The reaction of this La(OTf)$_3$ material with Me$_3$tach in THF led to isolation of [HMe$_3$tach][(Me$_3$tach)$_2$La(OTf)$_4$], **6-La**, Fig. 6, eqn (5), which has four anionic ligands in between two Me$_3$tach rings. The countercation balancing the charge of the [(Me$_3$tach)$_2$La(OTf)$_4$]$^{1-}$ anion is a protonated $[HMe_3tach]^{1+}$ moiety. The hydrogen atoms on the $[HMe_3tach]^{1+}$ could be refined and a hydrogen was located on N(7), which forms a hydrogen bonding ineraction to an oxygen atom in a triflate moiety containing O(4). Furthermore, the 1.484(5)–1.535(5) Å N–C distances involving protonated N(7) are longer than the 1.428(5)–1.466(5) Å N–C distances of other nitrogen atoms in the $[HMe_3tach]^{1+}$ moiety (see ESI for full details). Formation of $[HMe_3tach]^{1+}$ cations readily occurs,[50–52] as described in a later section, and is clearly a hinderance to Me_3tach chemistry with rare-earth metals in that it complicates reactions. The bulk synthesis of **6-La** was not pursued further. **6-La** is readily soluble in both THF and toluene despite being a cation-anion pair. This is likely due to the triflate anions which typically afford better solubility in rare-earth metal complexes than halide compounds.

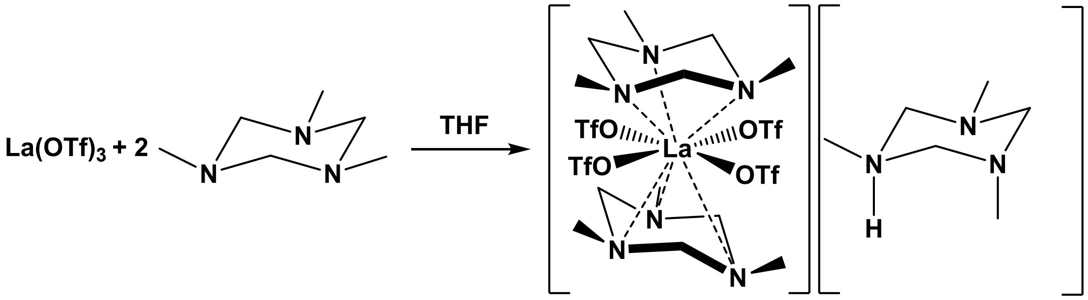

(5)

6-La

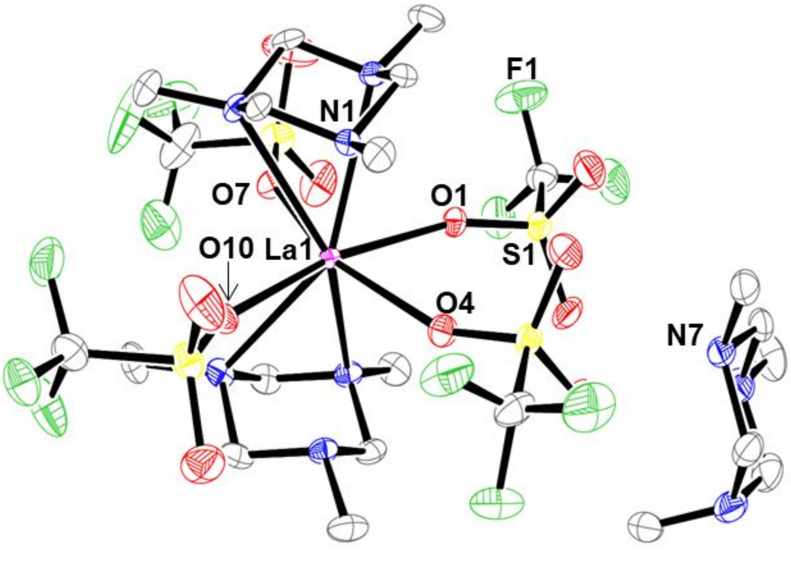

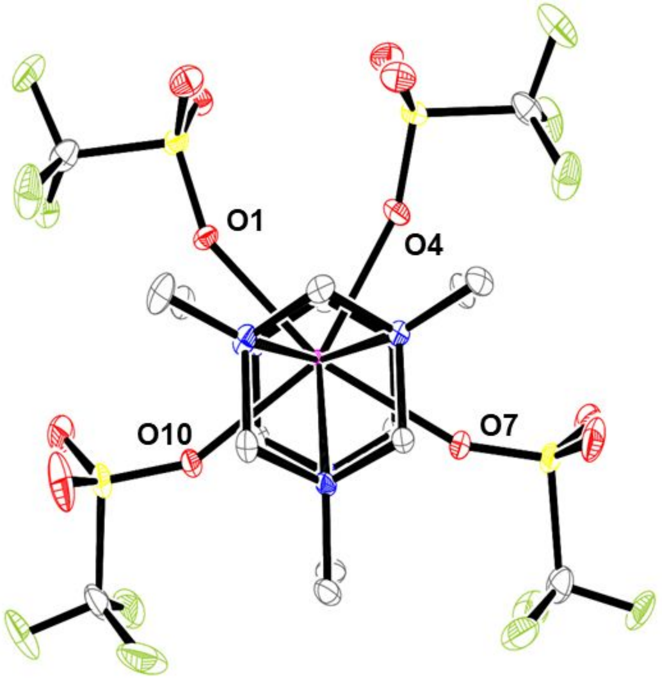

Fig. 6 Molecular structure of **6-La** (top), and a top-down view of the anion of **6-La** (bottom) with selective atom labelling. Ellipsoids are drawn at the 50% probability level and hydrogen atoms have been omitted for clarity.

The structure of **6-La** differs from that of **1-Ln** and **3-La** in that the Cnt–La–Cnt angle is bent at 163.1°. Three of the O–La–O angles that involve adjacent $(OTf)^{1-}$ units are similar to each other at 77.06(2), 79.21(7), and 87.05(8)°. However, the fourth angle O(7)–La–O(10) is 116.69(7)° which opens up the space where the two Me_3tach rings bend toward each other. The La–Cnt distances in **6-La** are very similar at 2.449 and 2.454 Å, which are similar to the 2.428 Å distance in **3-La**. The canting of the Me_3tach rings leads to 83.3–87.0° Cnt–La–O(OTf) angles for O(7) and O(10), and 92.5–99,6° angles for O(1) and O(4).

Reaction of Me_3tach with SmI_2. In addition to the exploratory reactions with Ln(III) precursors, the common Sm(II) reagent $SmI_2(THF)_x$ was examined. The reaction of $SmI_2(THF)_x$ (x = 0, 2)[53,54] with Me_3tach in THF formed a dark green solution. If the reaction is worked up within two hours, the red Sm(II) compound $(Me_3tach)_2SmI_2(THF)$, **7-Sm**, can be isolated, eqn (6), and identified by X-ray crystallography. **7-Sm** is readily soluble in THF, but surprisingly insoluble in toluene. In a reaction allowed to stir overnight, the green color fades to yellow and the Sm(III) compound [(Me$_3$tach)$_2$SmI$_2$][I], **2-Sm**, analogous to **2-Nd**, was isolated and identified by X-ray diffraction, eqn (6), Fig. 2. The isolation of the Sm(III) compound **2-Sm** is in contrast to the studies with Sm(AlMe$_4$)$_3$, which formed Sm(II) products in reactions with R$_3$tach.[29,35,37] A bulk synthesis of **2-Sm** was not attempted, but could likely be achieved in the same manner as eqn (2).

Compound **7-Sm** crystallizes in the *Pnma* space group with only half of the molecule present in the asymmetric unit. Unfortunately, the crystal data were such that only the connectivity of the molecule could be established. Compound **2-Sm** crystallizes in the *P*2$_1$/*m* space group, which is different than **2-Nd** which crystallizes in the *P*2$_1$/*c* space group, but again the crystal data were not of sufficient quality to discuss metrical parameters.

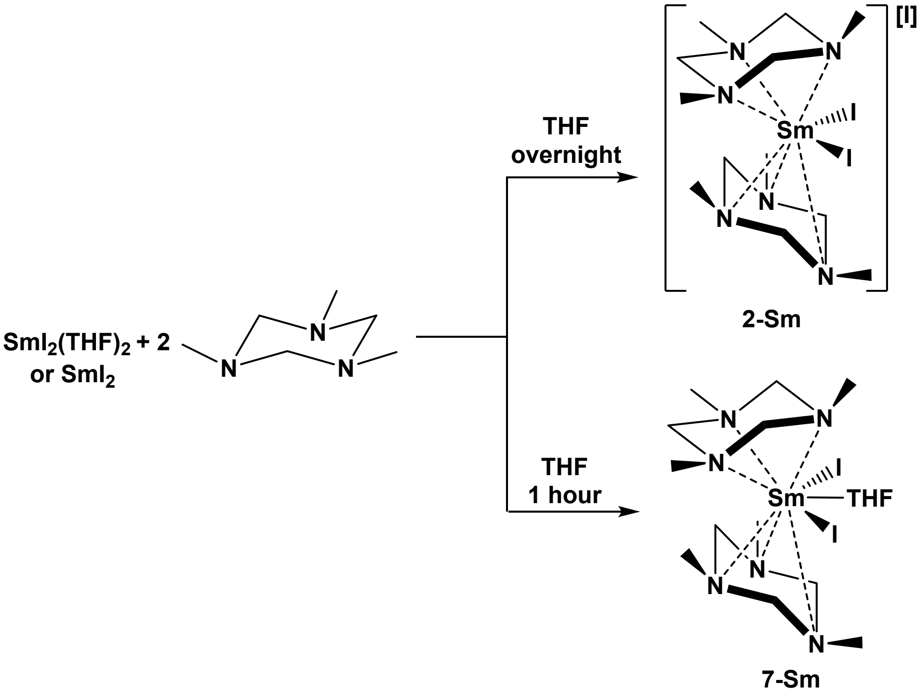

(6)

Me$_3$tacn Reactions. With LaI$_3$(THF)$_4$. For comparison with the Me$_3$tach results above, some reactions of rare-earth metal halides with the larger Me$_3$tacn ligand were investigated. Since the reaction of *one* equivalent of Me_3tach and $LaI_3(THF)_4$ forms a product with *two* tridentate ligands, $(Me_3tach)_2LaI_3$, **1-La**, it was of interest to determine if a complex with a single tridentate donor would form with the larger Me_3tacn ligand. Indeed, the reaction of $LaI_3(THF)_4$ with Me_3tacn in THF led to the formation of the mono(triazacycloalkane) product, $(Me_3tacn)LaI_3(THF)$, **8-La**, Fig. 7, eqn (7). Even if a four-fold excess of Me_3tacn was used, only the mono(chelate) **8-La** was isolated. **8-La** is readily soluble in THF and moderately soluble in toluene. The ^{1}H NMR spectrum of **8-La** in THF-d_8 displayed three resonances, attributable to inequivalent methylene protons and the methyl groups. The methylene resonances exhibited a complicated splitting pattern that could not be readily assigned.

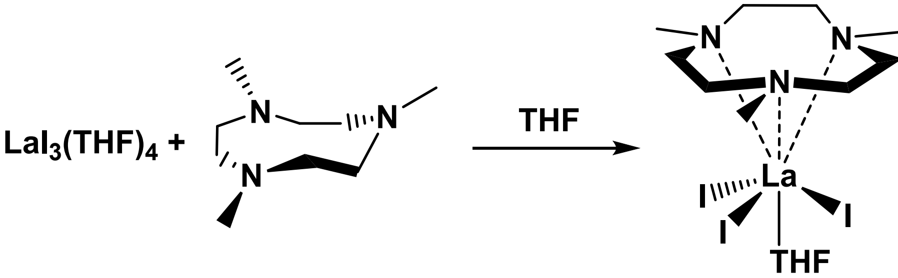

(7)

8-La
14% crystalline yield

Compound **8-La** crystallizes in the *Pna*2_1 space group and is isomorphous with the uranium analog $(Me_3tacn)UI_3(THF)$.[43] One THF molecule is coordinated to the lanthanum center in the solid state. The lanthanum center is 0.859 Å out of the plane formed by the three iodine atoms. The Cnt–La–O angle is nearly linear at 171.6°. The Cnt–La distance is 2.129 Å, which is shorter than the 2.185 Å distance in $(Me_3tacn)La(4\text{-methylbenzyl})_3$[41] and significantly shorter than the analogous distances in the lanthanum Me_3tach complexes: 2.428 Å in **3-La** and 2.449 and 2.454 Å in **6-La**. The closer contact of the chelate with the metal center for Me_3tacn versus Me_3tach has been observed in previous studies with **1-An**[43] and with Bi complexes.[44] This has been attributed to the fact that the Me_3tacn ligand is more flexible than Me_3tach due to the ethylene linkers and can approach the metal closer. A comprehensive list of Me_3tacn rare-earth metal complexes is tabulated in Table S2 the ESI and consistently show shorter M–Cnt distances than analogous Me_3tach complexes. The M–Cnt distances trend with the ionic radius of the metal and there is little variance when the ionic radius is accounted for.

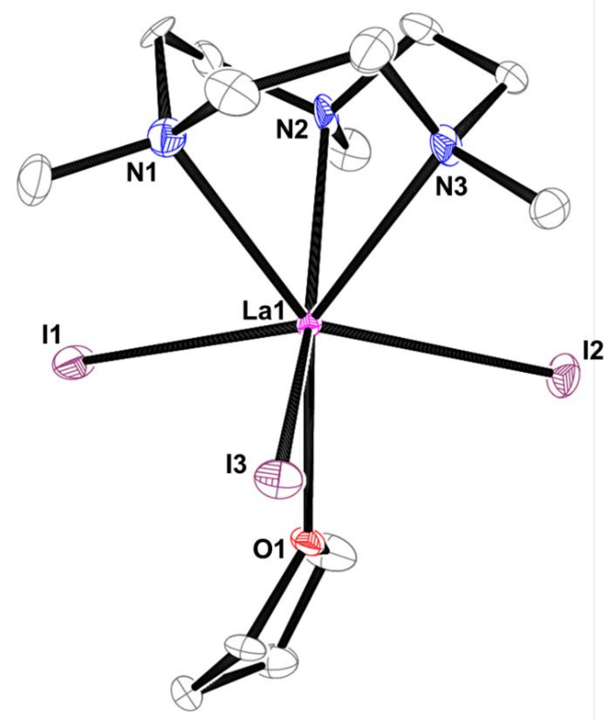

Fig. 7 Molecular structure of **8-La** with selective atom labelling. Ellipsoids are drawn at the 50% probability level and hydrogen atoms have been omitted for clarity.

With YCl_3. The reaction of YCl_3 with Me_3tacn was examined for comparison with $(Me_3tach)YCl_3(THF)_2$, **4-Y**. YCl_3 reacts with Me_3tacn in THF to form toluene soluble $(Me_3tacn)YCl_3$, **9-Y**, Fig. 8, eqn (8). **9-Y** is readily soluble in both THF and toluene. The ^{1}H NMR spectrum of **9-Y** in THF-d_8 displayed similar resonances to **8-La** above; three resonances were observed with the methylene resonances displaying a complicated splitting pattern. As in the La examples above, the 1.853 Å Cnt–Y distance in **9-Y** is shorter than the 2.214 Å Cnt–Y distance in **4-Y**. With the larger Me_3tacn ligand binding closer to the yttrium center, no THF molecules are bound to the metal, compared to two found in the Me_3tach complex **4-Y**. The result is a structure resembling a classic piano stool complex incorporating the Me_3tach ligand in place of a cyclopentadienyl ligand.

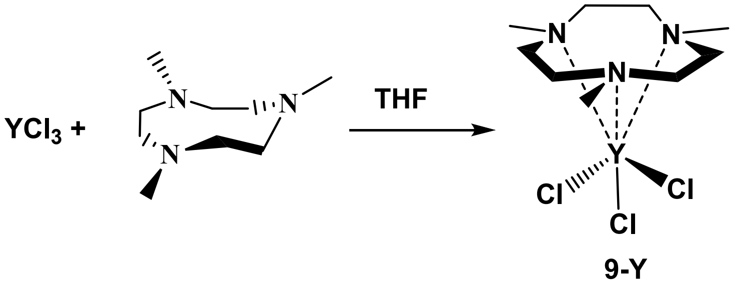

(8)

9-Y
14% crystalline yield

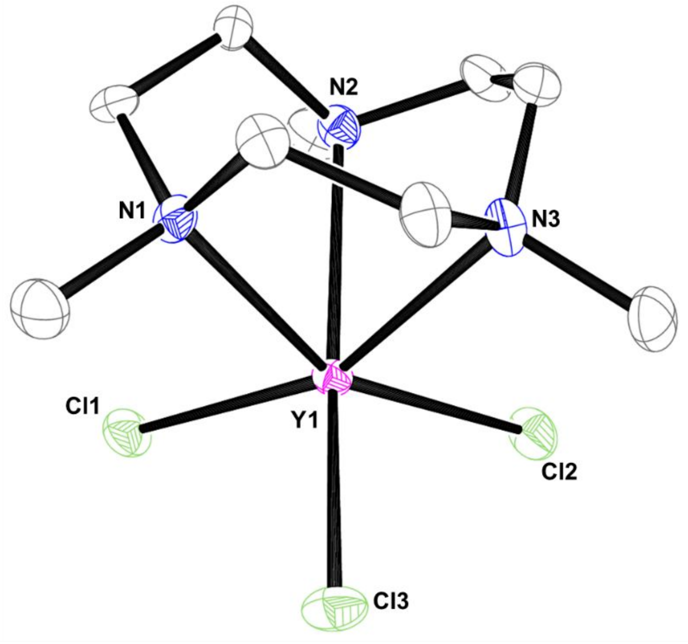

Fig. 8 Molecular structure of **9-Y** with selective atom labelling. Ellipsoids are drawn at the 50% probability level and hydrogen atoms have been omitted for clarity.

With $SmI_2(THF)_2$. The reaction of $SmI_2(THF)_2$ with Me_3tacn in THF led to the isolation of the mono-ring complex, $(Me_3tacn)SmI_2(THF)$, **10-Sm**, eqn (9), in contrast to the bis(Me_3tach) product, $(Me_3tach)_2SmI_2(THF)$, **7-Sm**, eqn (6). Like **9-Y**, a three-legged piano stool structure is observed.

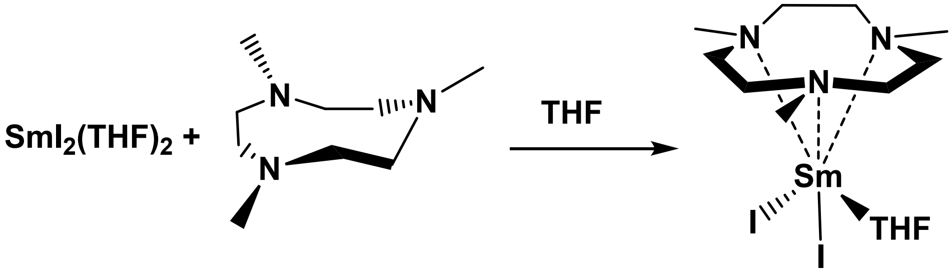

(9)

10-Sm
18% crystalline yield

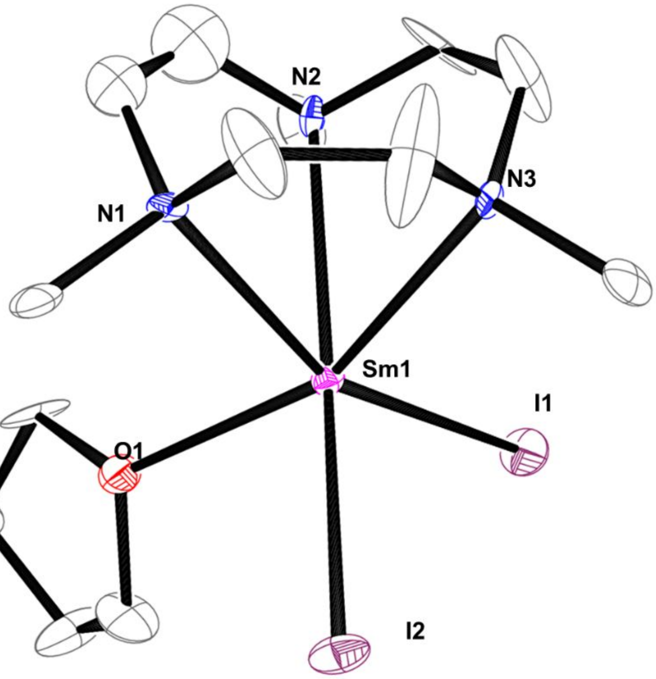

Fig. 9 Molecular structure of **10-Sm** with selective atom labelling. Ellipsoids are drawn at the 50% probability level and hydrogen atoms have been omitted for clarity.

Protonation of Me_3tach and Me_3tacn. Throughout these studies, protonated trimethyltriazacycloalkane byproducts were sometimes isolated from the reaction mixtures. As described above, the countercation in **6-La** was a $[HMe_3tach]^{1+}$ cation, eqn (5). In several cases, crystals of the protonated trimethyltriazacycloalkane were obtained which had the corresponding anion of the starting material as the counter anion. Specifically, the crystal structures of [HMe$_3$tach][Cl], [HMe$_3$tach][Br], [HMe$_3$tach][I], and [HMe$_3$tacn][OTf] were collected during these studies. Complete metrical data for [HMe$_3$tach][Br] is described in the ESI. The [HMe$_3$tach]$^{1+}$ structures revealed hydrogen bonding between the N–H proton and the corresponding anion. Protonated Me$_3$tach and Me$_3$tacn compounds have been previously observed.[50–52]

Discussion

Both Me$_3$tach and Me$_3$tacn readily coordinate to simple rare-earth metal salts that are common starting materials. A variety of structures were observed in this study depending on the nitrogen chelate, the metal size, and the anionic ligands present. A diversity of structures was also observed with bismuth halides and Me$_3$tach and Me$_3$tacn.[44] The Me$_3$tach ligand tends to form bis(chelate) complexes, although the mono-chelate (Me$_3$tach)YCl$_3$(THF)$_2$ can be isolated. In the case of the larger Me$_3$tacn ligand, only mono(chelate) complexes were observed in this study. It is likely that more variations in structure are accessible by adjusting the reactions conditions and reaction times. The isolation of both (Me$_3$tach)$_2$NdI$_3$, **1-Nd**, with parallel Me$_3$tach ligands, and [(Me$_3$tach)$_2$NdI$_2$][I], **2-Nd**, with a bent arrangement of ligands, is a good example. The interchangeability of these two structural forms suggests that many structural variations could be energetically accessible depending on conditions. This flexibility of Me$_3$tach in coordination can make it valuable in a variety of systems.

From the data collected here, it appears that iodide starting materials LnI$_3$(THF)$_x$ are the best candidates to coordinate Me$_3$tach to form THF-free, toluene soluble compounds which could be used as alternative precursors in ether-free reactions, like what has observed for the analogous **1-U** compound.[40] The chloride compound, (Me$_3$tach)$_2$LaCl$_3$, **3-La**, was much less soluble than the analogous iodide compounds $(Me_3tach)_2LnI_3$, **1-Ln**, and the triflate reactions showed that residual proton sources can be problematic in Me_3tach reactions as in the formation of $[HMe_3tach][(Me_3tach)_2La(OTf)_4]$, **6-La**. Protonation of Me_3tach (as well as Me_3tacn) can be a problem in general for all these reactions. Since Me_3tach is currently less expensive than Me_3tacn, it would be the preferred reagent to form toluene soluble compounds.

More generally, Me_3tach should be useful to coordinate rare-earth metal ions whenever addition ligation is needed. A previously published example of the utility of Me_3tach is its reaction with $\{[(C_5Ph_3H_2)TbCl_2(THF)]_2(KCl)(THF)\}_4$ that breaks up the tetramer and forms the monometallic compound $(C_5Ph_3H_2)TbCl_2(Me_3tach)$.[38] Me_3tach also could be added to compounds that do not readily crystallize to aid in purification and isolation of these species. The flexibility in coordination modes for Me_3tach should be an advantage in such endeavors.

Conclusions

Me_3tach readily coordinates to $LnI_3(THF)_x$ (Ln = La, Ce, Nd, Sm), $LaCl_3$, and $La(OTf)_3$ to generate $(Me_3tach)_2LnI_3$, **1-Ln**, $(Me_3tach)_2LaCl_3$, **3-La**, and $[(Me_3tach)_2La(OTf)_4]^{1-}$, **6-La**. The formation of the toluene soluble compounds such as **1-Ln** suggests that combinations of Me_3tach with lanthanide triiodides may provide good precursors for THF-free reactions. The Me_3tach ligand shows considerable flexibility in coordination and forms bis(Me_3tach) complexes with both parallel rings and bent structures as well as mono(Me_3tach) species. Comparative studies with Me_3tacn show that this larger ring can bind closer to the rare-earth metal ions and tends to form mono(ring) complexes. Me_3tach and Me_3tacn also coordinate to SmI_2 to form new Sm(II) derivatives. Although Me_3tach is prone to protonation and compounds containing $[HMe_3tach]^{1+}$

can readily form, this ligand is a good, inexpensive option for derivatization of rare-earth metal complexes.

ASSOCIATED CONTENT

Electronic Supplementary Information is available: Experimental details, crystallographic data, and NMR spectra. See DOI: 10.1039/x0xx00000x

Accession codes

CCDC 2236565–2236571 and 2244010 contain the supplementary crystallographic data for this paper. These data can be obtained free of charge via www.ccdc.cam.ac.uk/data_request/cif, or by emailing data_request@ccdc.cam.ac.uk, or by contacting The Cambridge Crystallographic Data Centre, 12 Union Road, Cambridge CB2 1EZ, UK; fax: +44 1223 336033.

Author Information

Justin C. Wedal: 0000-0003-0437-8601

Joseph W. Ziller: 0000-0001-7404-950X

William J. Evans: 0000-0002-0651-418X

Conflicts of Interest

The authors declare no competing financial interest.

ACKNOWLEDGMENTS

We thank the U.S. National Science Foundation for support under CHE-2154255. We also would like to thank Sierra R. Ciccone for the generous donation of $SmI_2(THF)_2$.

References

1 J. C. Wedal and W. J. Evans, *J. Am. Chem. Soc.*, 2021, **143**, 18354–18367.

2 W. J. Evans, *Organometallics*, 2016, **35**, 3088–3100.

3 H. Schumann and W. Genthe, in *Handbook on the Physics and Chemistry of Rare Earths*, eds. K. A. Gschneidner Jr. and L. Eyring, Elsevier B.V., 1984, pp. 445–571.

4 G. R. Willey, T. J. Woodman, U. Somasundaram, D. R. Aris and W. Errington, *J. Chem. Soc., Dalton Trans.*, 1998, **2**, 2573–2576.

5 D. C. Bradley, D. M. Frigo, I. S. Harding, M. B. Hursthouse and M. Motevalli, *J. Chem. Soc., Chem. Commun.*, 1992, 577–578.

6 K. Wieghardt, *Pure Appl. Chem.*, 1988, **60**, 509–516.

7 L. F. Lindoy, in *Macrocyclic Chemistry*, ed. K. Gloe, Springer, Dordrecht, 2005, pp. 53–66.

8 E. Macedi, A. Bencini, C. Caltagirone and V. Lippolis, *Coord. Chem. Rev.*, 2020, **407**, 213151.

9 P. Chaudhuri and K. Wieghardt, in *Progress in Inorganic Chemistry*, ed. S. J. Lippard, John Wiley & Sons, Inc., 2007, pp. 329–436.

10 M. Everett, A. Jolleys, W. Levason, M. E. Light, D. Pugh and G. Reid, *Dalton Trans.*, 2015, **44**, 20898–20905.

11 K. Wieghardt, M. Kleine-Boymann, B. Nuber and J. Weiss, *Inorg. Chem.*, 1986, **25**, 1309–1313.

12 F. Cheng, A. L. Hector, W. Levason, G. Reid, M. Webster and W. Zhang, *Chem. Commun.*, 2009, **3**, 1334.

13 F. Cheng, M. F. Davis, A. L. Hector, W. Levason, G. Reid, M. Webster and W. Zhang, *Eur.*

J. Inorg. Chem., 2007, **2007**, 4897–4905.

14 G. R. Willey, D. R. Aris, J. V. Haslop and W. Errington, *Polyhedron*, 2001, **20**, 423–429.

15 G. R. Willey, D. R. Aris, A. L. Beaumont and W. Errington, *Main Gr. Met. Chem.*, 1999, **22**, 515–518.

16 G. R. Willey, M. P. Spry and M. G. B. Drew, *Polyhedron*, 1996, **15**, 4497–4500.

17 F. Cheng, A. L. Hector, W. Levason, G. Reid, M. Webster and W. Zhang, *Angew. Chem. Int. Ed.*, 2009, **48**, 5152–5154.

18 B. Biswas, S. Salunke-Gawali, T. Weyhermüller, V. Bachler, E. Bill and P. Chaudhuri, *Inorg. Chem.*, 2010, **49**, 626–641.

19 A. Majumdar and R. H. Holm, *Inorg. Chem.*, 2011, **50**, 11242–11251.

20 N. L. Armanasco, M. V. Baker, M. R. North, B. W. Skelton and A. H. White, *J. Chem. Soc., Dalton Trans.*, 1998, **6**, 1145–1150.

21 D. V. Partyka, R. J. Staples and R. H. Holm, *Inorg. Chem.*, 2003, **42**, 7877–7886.

22 M. V. Baker, M. R. North, B. W. Skelton and A. H. White, *Inorg. Chem.*, 1999, **38**, 4515–4521.

23 H. Braband, S. Imstepf, M. Felber, B. Spingler and R. Alberto, *Inorg. Chem.*, 2010, **49**, 1283–1285.

24 F. T. Edelmann, D. M. M. Freckmann and H. Schumann, *Chem. Rev.*, 2002, **102**, 1851–1896.

25 W. E. Piers and D. J. H. Emslie, *Coord. Chem. Rev.*, 2002, **233**–**234**, 131–155.

26 P. M. Zeimentz, S. Arndt, B. R. Elvidge and J. Okuda, *Chem. Rev.*, 2006, **106**, 2404–2433.

27 S. Arndt and J. Okuda, *Adv. Synth. Catal.*, 2005, **347**, 339–354.

28 P. Mountford and B. D. Ward, *Chem. Commun.*, 2003, **3**, 1797.

29 D. Bojer, B. Neumann, H. Stammler and N. W. Mitzel, *Chem. – Eur. J.*, 2011, **17**, 6239–6247.

30 C. S. Tredget, S. C. Lawrence, B. D. Ward, R. G. Howe, A. R. Cowley and P. Mountford, *Organometallics*, 2005, **24**, 3136–3148.

31 D. Bojer, A. Venugopal, A. Mix, B. Neumann, H. Stammler and N. W. Mitzel, *Chem. – Eur. J.*, 2011, **17**, 6248–6255.

32 A. Nieland, J.-H. Lamm, A. Mix, B. Neumann, H.-G. Stammler and N. W. Mitzel, *Z. Anorg. Allg. Chem.*, 2014, **640**, 2484–2491.

33 A. Venugopal, I. Kamps, D. Bojer, R. J. F. Berger, A. Mix, A. Willner, B. Neumann, H.-G. Stammler and N. W. Mitzel, *Dalton Trans.*, 2009, 5755–5765.

34 R. D. Köhn, Z. Pan, G. Kociok-Köhn and M. F. Mahon, *J. Chem. Soc., Dalton Trans.*, 2002, 2344–2347.

35 D. Bojer, B. Neumann, H. Stammler and N. W. Mitzel, *Eur. J. Inorg. Chem.*, 2011, **2011**, 3791–3796.

36 M. Niemeyer, J. Christoffers and M. Rössle, *Acta Crystallogr. Sect. E Struct. Reports Online*, 2005, **61**, m1207–m1209.

37 D. Bojer, A. Venugopal, B. Neumann, H.-G. Stammler and N. W. Mitzel, *Angew. Chem. Int. Ed.*, 2010, **49**, 2611–2614.

38 D. A. Bardonov, P. D. Komarov, V. I. Ovchinnikova, L. N. Puntus, M. E. Minyaev, I. E. Nifant'ev, K. A. Lyssenko, V. M. Korshunov, I. V. Taidakov and D. M. Roitershtein, *Organometallics*, 2021, **40**, 1235–1243.

39 B. J. Hellmann, I. Kamps, A. Mix, B. Neumann, H.-G. Stammler and N. W. Mitzel, *Chem. Commun.*, 2010, **46**, 6536–6538.

40 A. A. Vinogradov, K. A. Lysenko, I. V. Anan'ev, I. E. Nifant'ev and D. M. Roitershtein, *Russ. J. Coord. Chem.*, 2020, **46**, 308–316.

41 S. Bambirra, A. Meetsma and B. Hessen, *Acta Crystallogr. Sect. E Struct. Reports Online*, 2007, **63**, m2891–m2891.

42 H. L. Buckley, M. R. Anstey, D. T. Gryko and J. Arnold, *Chem. Commun.*, 2013, **49**, 3104–3106.

43 J. C. Wedal, J. Murillo, J. W. Ziller, B. L. Scott, A. J. Gaunt and W. J. Evans, *Inorg. Chem.*, 2022, *in press*, DOI:10.1021/acs.inorgchem.2c03306.

44 J. C. Wedal, J. W. Ziller and W. J. Evans, *Inorg. Chem.*, 2022, **61**, 11766–11774.

45 E. L. Muetterties, *Tetrahedron*, 1974, **30**, 1595–1604.

46 J. C. Wedal, C. J. Windorff, D. N. Huh, A. J. Ryan, J. W. Ziller and W. J. Evans, *J. Coord. Chem.*, 2021, **74**, 74–91.

47 J. C. Wedal, J. W. Ziller, F. Furche and W. J. Evans, *Inorg. Chem.*, 2022, **61**, 7365–7376.

48 H. Schumann, J. A. Meese-Marktscheffel and L. Esser, *Chem. Rev.*, 1995, **95**, 865–986.

49 R. D. Shannon, *Acta Crystallogr. Sect. A*, 1976, **32**, 751–767.

50 R. D. Köhn, M. Haufe, G. Kociok-Köhn and A. C. Filippou, *Inorg. Chem.*, 1997, **36**, 6064–6069.

51 G. R. Willey, L. T. Daly, P. R. Meehan and M. G. B. Drew, *J. Chem. Soc., Dalton Trans.*, 1996, 4045–4053.

52 G. R. Willey, D. R. Aris, W. Aemaeg and W. Errington, *Inorg. Chim. Acta*, 2001, **317**, 304–313.

53 P. Girard, J. L. Namy and B. Kagan, *J. Am. Chem. Soc.*, 1980, **102**, 2693–2698.

54 F. Ortu, *Chem. Rev.*, 2022, **122**, 6040–6116.